Received: 14 August 2021 | Revised: 08 October 2021 | Accepted: 01 November 2021
DOI: 10.22034/ecc.2021.299749.1217
Eurasian Chemical Communications
SAMI

FULL PAPER

Thermal stability, synthesis of new formazan complexes derived from thiophene-2-carboxaldehyde

Haneen H. Talib | **Jasim M. Alshawi***

Department of Chemistry, College of Education for Pure Sciences, University of Basrah, Iraq

A novel formazan ligand was prepared from the condensation of p-phenylenediamine and thiophene-2-carboxaldehyde with diazonium salt of 4-chloro aniline, and its metal transition complexes of Co (II), Cu (II) and Ni (II) were synthesized from the reaction of the metal chlorides with the formazan ligand in the molar ratio of 1:1 (M: L). The formazan ligand and its metal complexes were identified by different spectroscopic and analytical techniques. The results of this study suggested that the metal complexes had a tetrahedral geometry. Thermogravimetric analysis was used to study the thermal decomposition of the complexes. The results showed that all the steps were non-spontaneous, as evidenced by the positive ΔG values; the decomposition process was endothermic, as evidenced by the positive ΔH values; and the complexes were more ordered than the reactants, as evidenced by the negative ΔS values. The thermodynamic data (ΔH, ΔS, ΔG) were calculated by using the Coats-Redfern equation.

KEYWORDS

Formazan; thiophene-2-carboxaldehyde; complexes; p-phenylenediamine; 4-chloro aniline.

***Corresponding Author:**
Jasim M. Alshawi
Email: jasim.salih@uobasrah.edu.iq
Tel.: +00919652806704

Introduction

Formazans are an important and special class of organic compounds [1]. Their chemistry has attracted the attention of several researchers, who have used them for large biological studies and industrial applications [2], as well as in the preparation of heterocyclic compounds [3-5], and for analytical chemistry [6]. Formazans are utilized as analytical reagents for the spectroscopic identification of different metal ions due to their stable properties and intense colours [7]. They are coloured materials because of their π-π* transitions [8], and they have been identified as azohydrazones, due to their basic [-N=N-C(R)=N-NH-] structure, which is highly linked to the structure of azo dyes since they possess an azo functional group [9]. Their structure was first identified by Pechmann et al., who agreed to term them as formazyl compounds. In 1933, their utilization in Germany was exemplified by Beilstein, where the compounds were denoted as formazans. When a formazan compound is substituted by three phenyl groups (R, R′, R″), it is known as 1, 3, 5-triphenyl formazan [10]. Formazans are changed into tetrazolium salts upon oxidation, while tetrazolium compounds are reduced by the dehydrogenases of metabolically effective cells to produce formazans [11]. Formazans have been found to have significant medical applications due to their different properties, for example, antiviral [12], analgesic [13], antimicrobial [14], anticancer, anti-HIV [15], and antifungal

[16] properties. In this study, three new formazan complexes were prepared from the reaction between p-phenylenediamine and thiophene-2-carboxaldehyde with diazonium salt of 4-chloro aniline, and with dichloromethane as a solvent. All the complexes had a tetra-coordinated metal centre, and para-magnetic properties with sp^3 hybridization.

Experimental method

Instruments and spectral measurements

Infrared spectra were obtained using KBr pellets on an FTIR-84005-SHIMADZU. The ligand spectrum, ^{13}C-[^1H]- NMR, was obtained using a Bruker-100 HZ, and was recorded at room temperature in DMSO-d6 using TMS as reference material for all the spectra. The EI mass was done by using Agilent Technology (HP). The melting points were obtained using thermoscientific apparatus. The UV-visible range was measured using a T80+UV/VIS spectrometer (PG Instruments Ltd.) in the region of 200-800 nm with a 1 cm long quartz cell. The magnetic susceptibilities of the complexes were recorded using an auto-magnetic susceptibility balance, with glass tubes having a diameter of 0.324 cm. The thermogravimetric analysis was carried out using an STA 1500 Model (Rheometric Scientific Co.).

Methodology

The formazan ligand was prepared by the condensation of a Schiff base with diazonium salt of 4-chloro aniline.

Synthesis of schiff base A

0.2 g (0.001 mol) of thiophene-2-carboxaldehyde was dissolved in 10 mL of ethanol and mixed with 4-5 drops of glacial acetic acid. Next, 0.108 g (0.001 mol) of p-phenylenediamine was dissolved in 10 mL of ethanol and added gradually to an aldehyde solution under reflux. After 3 hours [17,18], it was filtered and recrystallized using ethanol (Scheme 1).

N,N′-(1,4-phenylene) bis (1-(thiophen-2-yl) methanimine); (A)

Yellow powder, yield 68%, M.P: 170-172 ^oC, ^1H-NMR (DMSO, 400 MHz, δ ppm), δ: 8.86 (N=C-H), δ: 7.38, 7.79 (C_7, C_8-H), respectively, δ: 7.66 (aromatic-H) (Figure 15). $^{13}CNMR$ (DMSO, 400 MHz, δ ppm), (153.7, 134, 143.07, 122.56) due to (C_4, (HC=N), C_6, (C-C), C_5, (C-S), Aromatic-C), respectively (Figure 17). MS: m/z: 296.1 [M^+]; 147.1 [M+]; 115.1 [M+] (Figure 10). IR (υ, cm^{-1}) 3068 (υ CH aromatic), 1603 (υ C=N), 1420 (υ C=C), 1350 (υ C-N) (Figure 1).

Synthesis of formazan ligand (L)

0.24 g (0.002 mol) of 4-chloroaniline was mixed with 7 mL of HCl and 3 mL of H_2O, while stirring in an ice bath until the temperature dropped below 5 ˚C. Next, 3 g (0.04 mol) of sodium nitrite was dissolved in distilled water. The prepared solution was then added gradually to the above solution to prepare the diazonium salt. Next, 0.29 g (0.0009 mol) of (A) and 0.17 g (0.0012 mol) of potassium carbonate were dissolved in dichloromethane [19], before being added gradually to the diazonium salt while stirring for 2 hours in an ice bath. The mixture was then filtered and recrystallized using ethanol (Scheme 1).

N,N′-(1,4-phenylene)bis(1-((4-chlorophenyl)diazenyl)-1-(thiophen-2-yl) methanimine) (L)

Walnut powder, yield 55%, M.P: 290-293 ˚C, ^1H-NMR (DMSO, 400 MHz, δ ppm), δ: 7.32, 7.41 (C_7, C_8-H), respectively, δ: 7.37 (aromatic-H) (Figure 16). ^{13}C-NMR (DMSO, 400 MHz, δ ppm), (156, 124.41, 134.3, 123.6) due to (C_4, (C=N), C_5, (C-S), C_{12}, (C-Cl), Aromatic-C), respectively (Figure 18). MS: m/z: 573.7 [M^+]; 551.6 [M+]; 495.5 [M+] (Figure 11). IR (υ, cm^{-1}) 3012 (υ CH

aromatic), 1660 (υ C=N), 1595 (υ N=N), 1388 (υ C-N) (Figure 2). UV-Visb, λ_{max} (ε): 274.6 nm (1990), 379.4 nm (1030) (Figure 6).

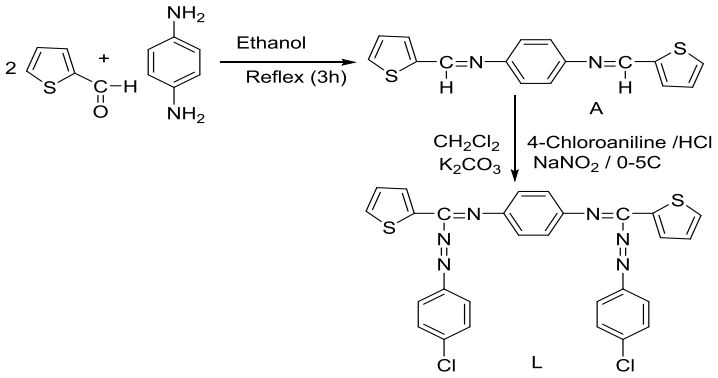

SCHEME 1 Synthesis of Schiff base (A) and ligand (L)

Synthesis of transition metal complexes (1-3)

0.22 g (0.0003 mol) of formazan L ($C_{28}H_{18}N_6S_2Cl_2$) in a mixture of ethanol:chloroform in the ratio of 3:1 mL, was respectively mixed with the metal chlorides (0.0003 mol) of $CuCl_2.2H_2O$, $CoCl_2.6H_2O$ and $NiCl_2.6H_2O$. This reaction was carried out by heating the mixture under reflux while stirring for three hours. The precipitate was separated out through filtration [20], and was then washed with diethyl ether (Scheme 2).

Complex 1[Cu (L)]Cl_2

Walnut powder; yield 46%; M.P.>300 ˚C, IR (υ, cm^{-1}) 3014 (υ CH aromatic), 1589 (υ C=N), 1504 (υ N=N), 445-487 (υ M-N) (Figure 3); UV-Visb, λ_{max} (ε): 228.2 nm (1440), 289.4 nm (1220), 578.1 nm (90) (Figure 7); MS: m/z: 637.5 [M^+]; 202.1 [M+]; 108.1 [M+] (Figure 12); molar conductance ($\Omega^{-1}.cm^2.mol^{-1}$) = 85; μ_{eff} (B.M.) = 1.801.

Complex 2 [Co (L)]Cl_2

Brown powder; yield 64%; M.P. >300 ˚C, IR (υ, cm^{-1}) 3050 (υ CH aromatic), 1654 (υ C=N), 1506 (υ N=N), 497-609 (υ M-N) (Figure 4); UV-Visb, λ_{max} (ε): 301.7 nm (610), 363.8 nm (360), 613.4 nm (90), 680 nm (80) (Figure 8); MS: m/z: 633.5 [M^+]; 602.7 [M+]; 563.5 [M+] (Figure 13); molar conductance ($\Omega^{-1}.cm^2.mol^1$) = 82; μ_{eff} (B.M.) = 2.389.

Complex 3 [Ni (L)]Cl_2

Grey powder; yield 55%; M.P. >300 ˚C, IR (υ, cm^{-1}) 3026 (υ CH aromatic), 1654 (υ C=N), 1492 (υ N=N), 453-540 (υ M-N) (Figure 5); UV-Visb, λ_{max} (ε): 259.7 nm (1410), 306.8 nm (540), 699.2 nm (30) (Figure 9); MS: m/z: 632.1 [M^+]; 207.2 [M+]; 111.2 [M+] (Figure 14); molar conductance ($\Omega^{-1}.cm^2.mol^{-1}$) = 90; μ_{eff} (B.M.) = 3.605.

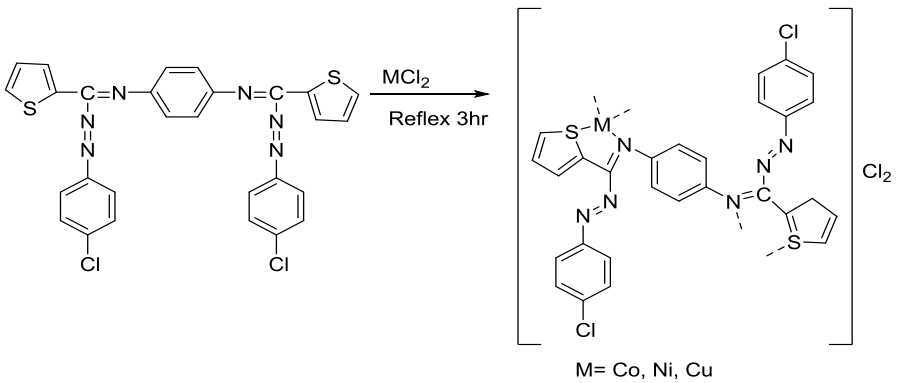

SCHEME 2 Proposed structure of the formazan ligand metal complexes 1-3

Results and discussion

A formazan ligand was prepared from the condensation of p-phenylenediamine and thiophene-2-carboxaldehyde with diazonium salt of 4-chloroaniline (Scheme 1). The transition metal complexes were synthesised from the reaction of formazan ligand with various transition metal salts ($CuCl_2.2H_2O$, $CoCl_2.6H_2O$, $NiCl_2.6H_2O$) in an ethanol:chloroform ratio of 3:1 as a solvent under reflux (Scheme 2). The complexes 1-3 were designed in accordance with a stoichiometric ratio of 1:1 (L: M). Based on the results of all the analytical studies, the metal complexes 1-3 were in agreement with the proposed general formula of $[ML]Cl_2$.

Characterization of formazan and complexes

The prepared compounds were characterised using spectroscopic techniques. The IR spectrum of the ligand showed a strong band at 1660 cm^{-1}, which was assigned to the (-C=N-) stretching vibration. Also, the bands at 1595, 1496 and 1388 cm^{-1} were assigned to the stretching vibrations of (N=N), (C=C) and (C-N), respectively. The IR spectra of the complexes showed strong bands at 1589-1654 cm^{-1}, which were assigned to the (-C=N) stretching vibration. The shifts in these complexes to lower wave numbers were compared with that of the free ligand, indicating that the nitrogen in the azomethine group had bonded with the metal ions to form coordinate bonds. The IR spectra showed bands at (1504-1506), (1494-1600), (1390-1404) cm^{-1}, which were assigned to the stretching vibrations of (N=N), (C=C) and (C-N), respectively. The IR spectra showed new bands at (445-609) cm^{-1}, which were assigned to (M-N) (Figures 1-5). The ^{1}HNMR spectrum of the ligand showed a triplet signal at δ 7.32 ppm, due to the (C_7-H); a doublet signal at δ 7.41 ppm, due to the (C_8-H); doublet of doublets signals at δ 8.06 and 8.16 ppm due to the (C_{10}, C_{11}-H), respectively; and a multiplet signal at 7.37 ppm, due to the aromatic-H (Figures 15 and 16). The ESl-mass spectra of the ligand (L) and its metal complexes (1-3) showed successive fragments related to the structures. The parent ion peak for the ligand observed at m/z 573.7 corresponded to the M+ ion for $C_{28}H_{18}N_6S_2Cl_2$, at m/z 573.5. The other peak fragments were shown at m/z 454.08 as (M+) for $C_{24}H_{15}ClN_6S$, and at m/z 489.05 08 as (M+) for $C_{24}H_{15}Cl_2N_6S$. These results were in agreement with the proposed formula for the ligand. The MS-ESI was also used to determine the molecular weights of the prepared compounds, where the molecular weights that were obtained were in accordance with the theoretical values (Figures 10-14). The elemental analyses were carried out for ligand and complexes and mathched values were found (Table 1).

Electronic spectra

The electronic spectra of the ligand exhibited two absorption bands at wavelengths 274.6 nm (ε=1990 $L.mol^{-1}.cm^{-1}$) and 379.4 nm (1030 $L.mol^{-1}.cm^{-1}$) due to the π—π* transition bands [21]. The electronic spectra of all the complexes exhibited absorption bands in the region of 228.2-363.8 nm (ε = 1440-360 $L.mol^{-1}.cm^{-1}$), which were attributed to the π—π* transition bands. Also, d-d transition bands were exhibited in the visible region, where the CuL showed a band at 578.1 nm (ε = 90 $L.mol^{-1}.cm^{-1}$), which was assigned to the $^3T_2 \rightarrow {}^3E$ band, while the CoL showed bands at 613.4 nm (ε = 90 $L.mol^{-1}.cm^{-1}$) and 680 nm (ε = 80 $L.mol^{-1}.cm^{-1}$), which were assigned to the $^4_FA_1 \rightarrow {}^4_pT_1$ and $^4_FA_2 \rightarrow {}^4T_1$, bands and the NiL showed a band at 699.2 nm (ε = 30 $L.mol^{-1}.cm^{-1}$), which was assigned to the $^3_FT_1 \rightarrow {}^3_pT_1$ band (Figures 6-9).

Thermal analysis

A thermal analysis technique known as thermogravimetry (TG) was used to obtain helpful data about the metal-ligand connection by studying the thermal action of

the transition metal complexes and their thermal decomposition. The thermogravimetric analysis of the complexes was conducted in an atmosphere of N_2, starting at room temperature to 600 ˚C, at an average heating rate of 10 ˚C/min [22].

Thermal degradation of [Cu($C_{28}H_{18}N_6S_2Cl_2$)]Cl2

The thermal degradation of [Cu($C_{28}H_{18}N_6S_2Cl_2$)]Cl_2 proceeded in three different stages. In the first stage, peaks were detected within the temperature range of 110-300 °C, indicating the loss of ($C_{31}H_{34}N_4Cl_4S_2$) (obs. = 3.06 mg; 94.3%. calc. = 3.68 mg, 94.4%). In the second stage, there was a weight loss (obs. = 3.4 mg; 89.2%. calc. = 3.50 mg, 89.7%) within the temperature range of 300-440 ˚C due to the removal of $C_{28}H_{32}N_4Cl_4S_2$. In the third stage, there was a weight loss (obs. = 3.2 mg; 84.5%. calc. = 3.30 mg, 84.61% within the temperature range of 440-590 ˚C due to the removal of $C_{25}H_{38}N_4Cl_4S_2$ (Figure 19).

Thermal degradation of [Co($C_{28}H_{18}N_6S_2Cl_2$)]Cl2

The thermal degradation of [Co($C_{28}H_{18}N_6S_2Cl_2$)]Cl_2 proceeded in three different stages. In the first stage, peaks were detected within the temperature range of 110-140 °C, indicating the loss of ($C_{31}H_{32}N_4Cl_4S_2$) (obs. = 12.6 mg; 94.7%. calc. = 12.7 mg, 94.8%). In the second stage, there was a weight loss (obs. = 12.08 mg; 90.2%. calc. = 12.1 mg, 90.3%) within the temperature range of 140-240 ˚C due to the removal of $C_{28}H_{36}N_4Cl_4S_2$. In the third stage, there was a weight loss (obs. = 11.4 mg; 85.81%. calc. = 11.5 mg, 85.82%) within the temperature range of 240-590 ˚C due to the removal of $C_{27}H_{18}N_4Cl_4S_2$ (Figure 20).

Thermal degradation of [Ni($C_{28}H_{18}N_6S_2Cl_2$)]Cl2

The thermal degradation of [Ni($C_{28}H_{18}N_6S_2Cl_2$)]Cl_2 proceeded in two different stages. In the first stage, peaks were detected within the temperature range of 290-400 °C, indicating the loss of ($C_{30}H_{38}N_4Cl_4S_2$) (obs.= 3.1 mg; 94.10%. calc. = 3.2 mg, 94.12%). In the second stage, there was a weight loss (obs. = 1.1 mg; 35.2%. calc. = 1.2 mg, 35.3%) within the temperature range of 400-580˚C due to the removal of $C_{10}H_{20}N_3ClS$ (Figure 21).

Kinetic and thermodynamic data analysis

The Coats-Redfern method (1) was employed to study the thermal decomposition of the complexes, and a summary of the thermal behaviour of the complexes is given in Table 2.

$$\log\left[\frac{\log\frac{Wf}{Wf-Wt}}{T^2}\right] = \log\left[\frac{AR}{\theta E}\left(1-\frac{2RT}{E}\right)\right] - \frac{E}{2.303\,RT} \quad (1)$$

where Wf denotes the weight loss at the end of the stage, Wt denotes the weight at any temperature. Also, E denotes the activation energy, R denotes the gas constant (8.314 $J.mol^{-1}.K^{-1}$), A denotes the pre-exponential factor, and θ denotes the heating rate of 10 ˚C/min.

E and A were calculated from the slope and intercept, respectively, while ΔH, ΔS and ΔG for all the steps were calculated using Equations (2-4),

$$\Delta H = \Delta E - RT \quad (2)$$

$$\Delta S = R \ln (Ah/K_BT_S) \quad (3)$$

$$\Delta G = \Delta H - T\Delta S \quad (4)$$

where *h* symbolizes Planck's constant ($6.6262x10^{-3}$ J.S); K_B denotes Boltzmann's constant ($1.3806x10^{-3}$ J/K), and T_S signifies maximum temperature. The results showed that the decomposition process was endothermic, as evidenced by the positive ΔH values; the complexes were more ordered than the reactants, as evidenced by the negative ΔS values; and the steps were non-spontaneous, as evidenced by the positive ΔG values (Figures 22 and 23).

TABLE 1 Elemental analysis of the ligand and complexes

Formula		C	H	N	M
$C_{16}H_{12}N_2S_2$	Calc.	64.84	4.08	9.45	
	Found	64.79	4.06	9.47	
$C_{28}H_{18}Cl_2N_6S_2$	Calc.	58.64	3.16	12.36	
	Found	58.61	3.13	12.40	
$C_{32}H_{32}Cl_4CoN_6S_2$	Calc.	50.20	4.21	10.98	7.70
	Found	50.18	4.19	11.01	7.71
$C_{32}H_{32}Cl_4CuN_6S_2$	Calc.	49.91	4.19	10.91	8.25
	Found	49.93	4.17	10.93	8.23
$C_{32}H_{32}Cl_4NiN_6S_2$	Calc.	50.22	4.21	10.98	7.67
	Found	50.25	4.23	11.02	7.66

TABLE 2 Kinetic parameters of the complexes using the Coats–Redfern equation

Complex	wt	Stage	A(1/S)	E(KJ/mol)	ΔH(KJ/mol)	ΔS(KJ/mol.K)	ΔG(KJ/mol)
$[Cu(C_{28}H_{18}N_6S_2Cl_2)]Cl_2$	3.9	1	-5.6697	4.31	1.6928	-27.2757	18.0275
		2	-6.1789	2.44	3.56875	-26.5606	15.63459
$[Co(C_{28}H_{18}N_6S_2Cl_2)]Cl_2$	13.4	1	-4.9259	0.96	5.04696	-28.4449	15.51869
		2	-4.6182	8.24	2.237922	-28.9811	23.19126
$[Ni(C_{28}H_{18}N_6S_2Cl_2)]Cl_2$	3.4	1	-4.4584	12.07	6.066423	-29.2739	27.23145

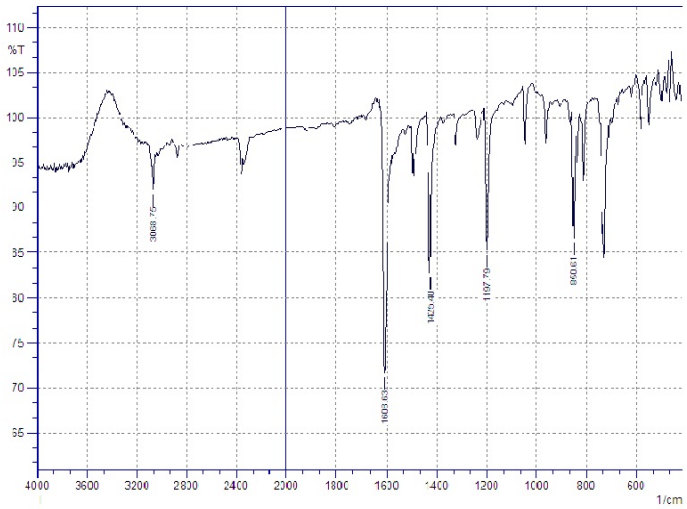

FIGURE 1 FT-IR spectrum of Schiff base (A)

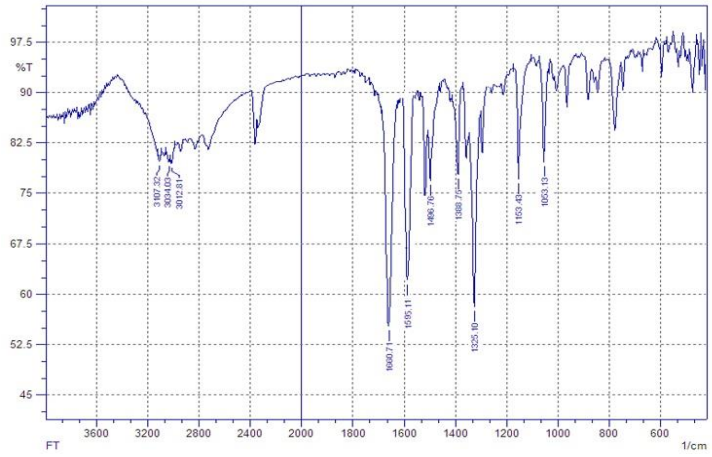

FIGURE 2 FT-IR spectrum of ligand (L)

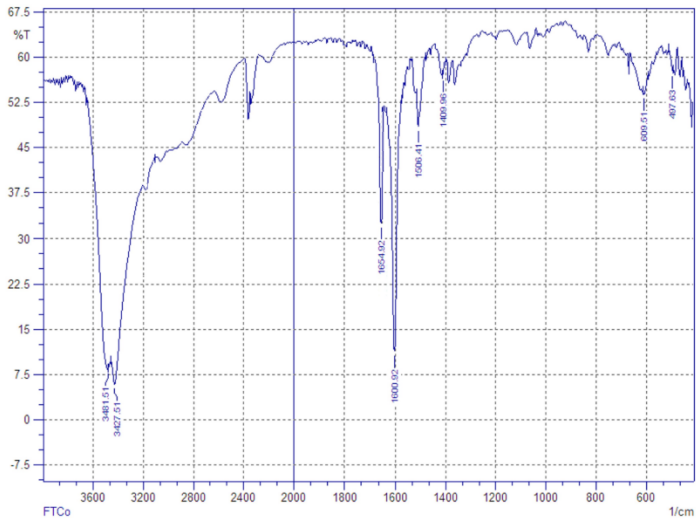

FIGURE 3 FT-IR spectrum of complex (1)

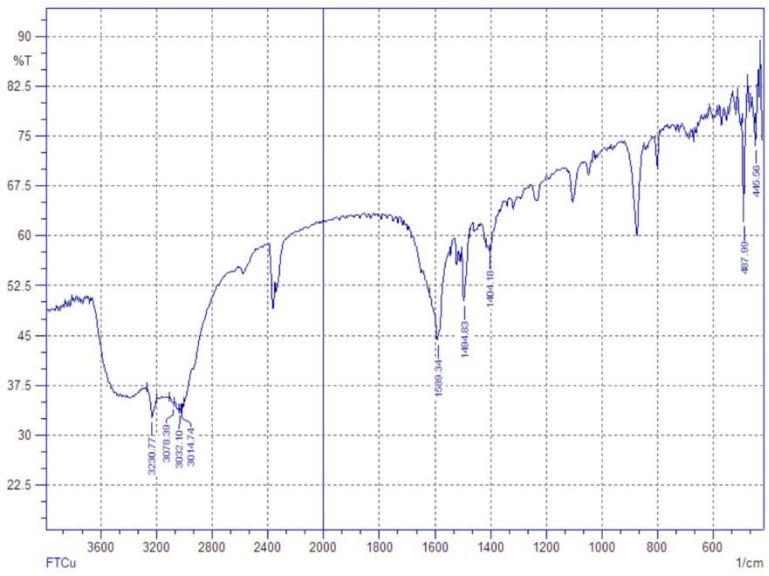

FIGURE 4 FT-IR spectrum of complex (2)

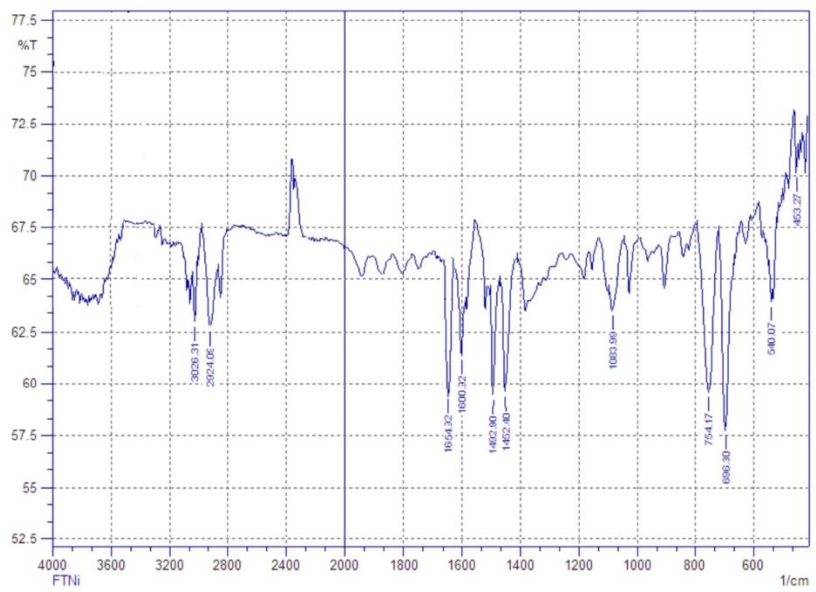

FIGURE 5 FT-IR spectrum of complex (3)

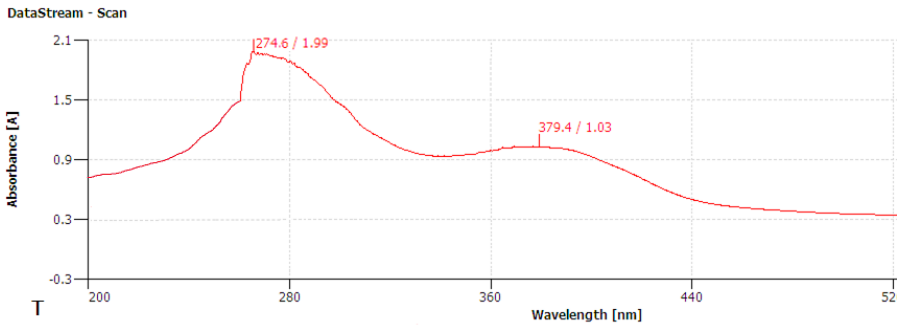

FIGURE 6 UV-Vis spectrum of (L)

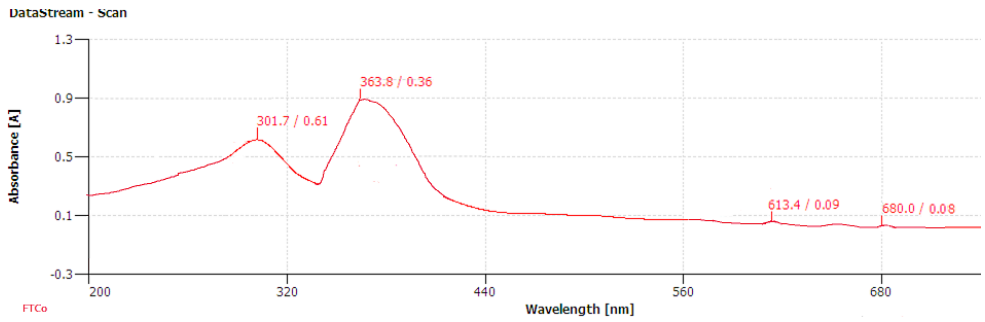

FIGURE 7 UV-Vis spectrum of complex (1)

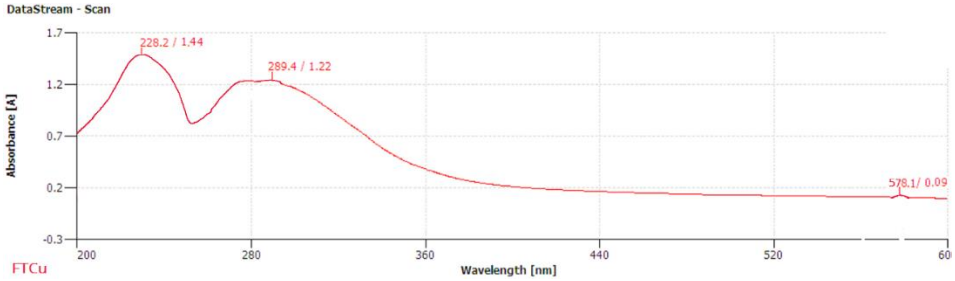

FIGURE 8 UV-Vis spectrum of complex (2)

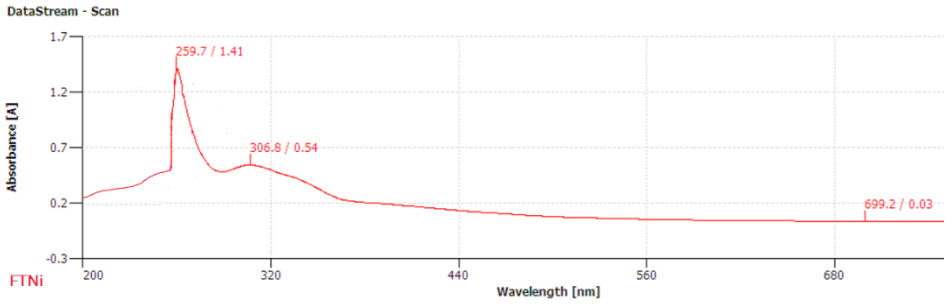

FIGURE 9 UV-Vis spectrum of complex (3)

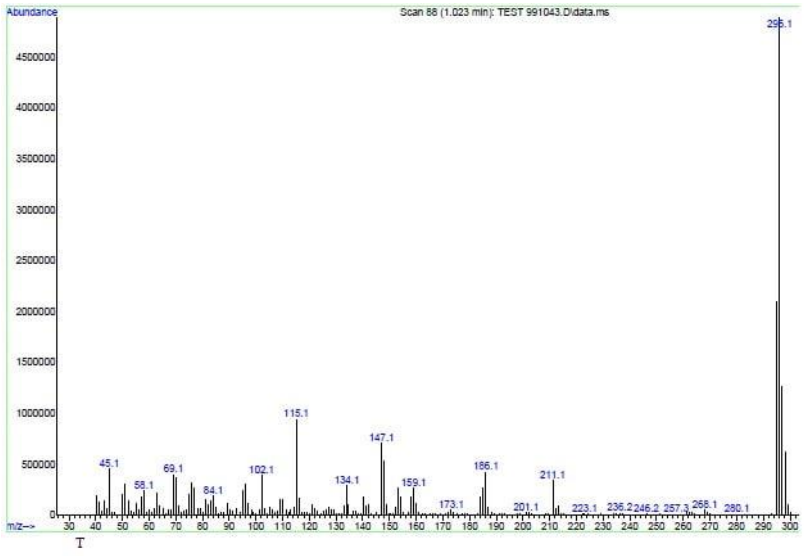

FIGURE 10 ESI-Mass spectrum of Schiff base (A)

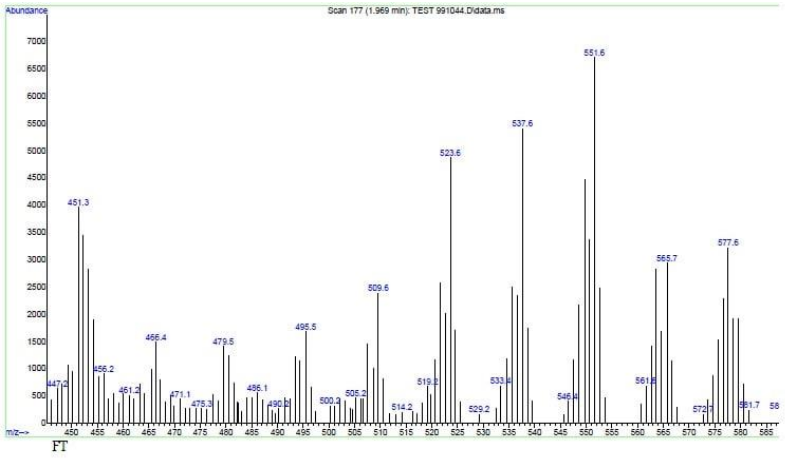

FIGURE 11 ESI-Mass spectrum of ligand (L)

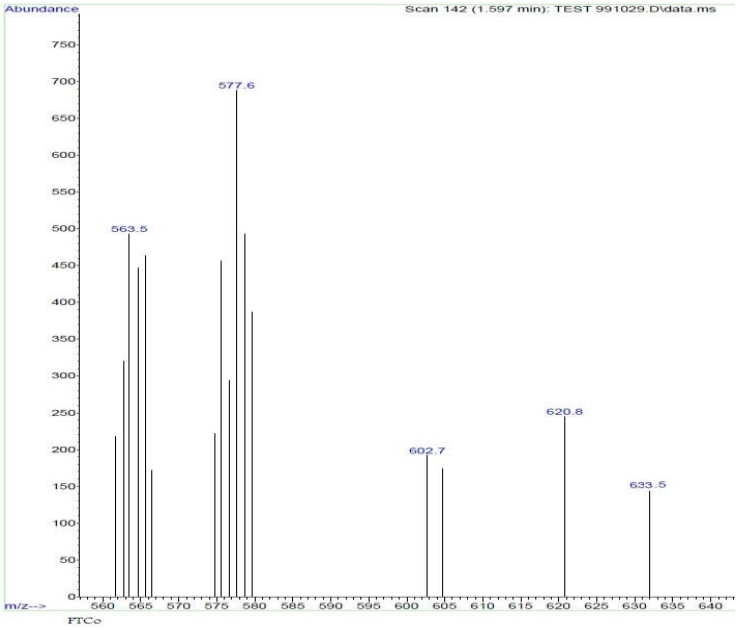

FIGURE 12 ESI-Mass spectrum of complex (1)

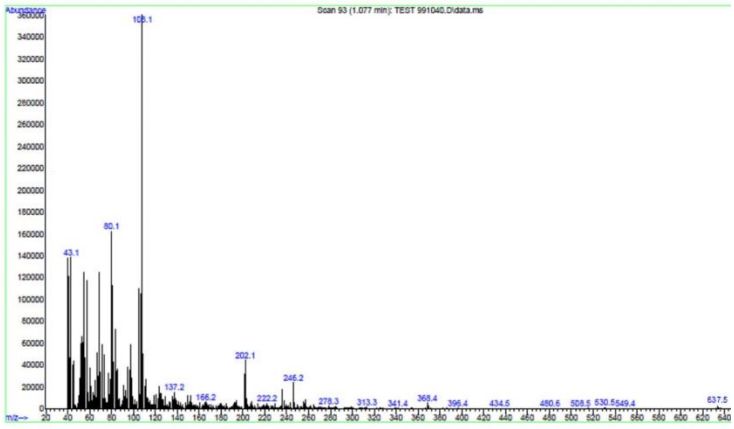

FIGURE 13 ESI-Mass spectrum of complex (2)

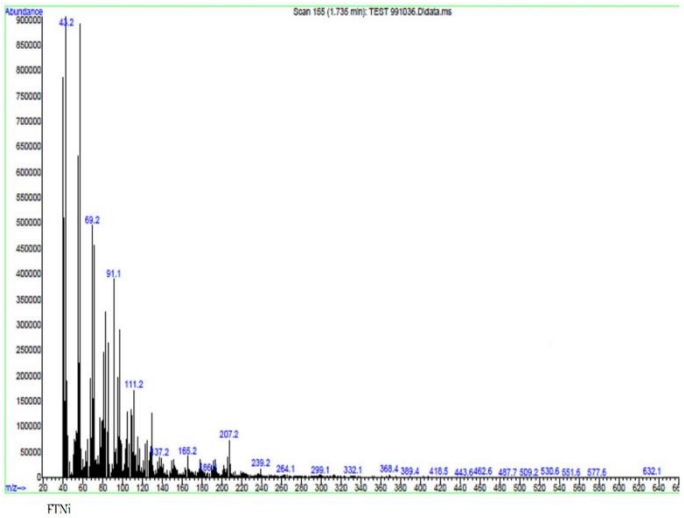

FIGURE 14 ESI-Mass spectrum of complex (3)

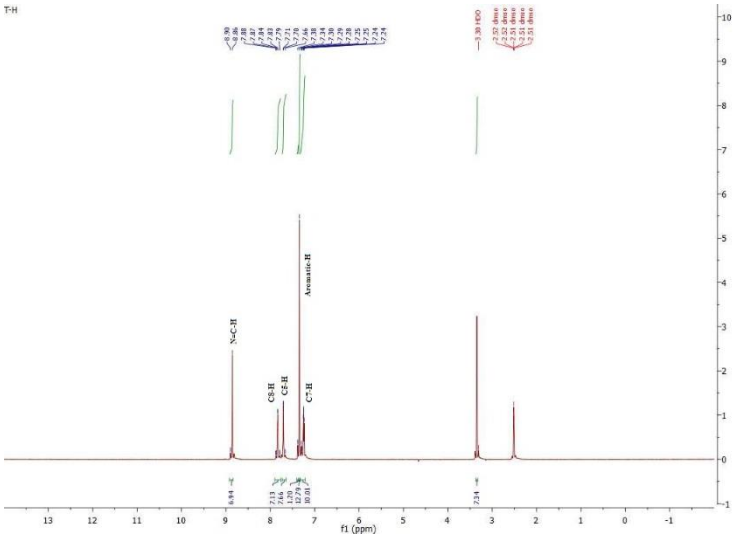

FIGURE 15 ^{1}H-NMR spectrum of Schiff base (A)

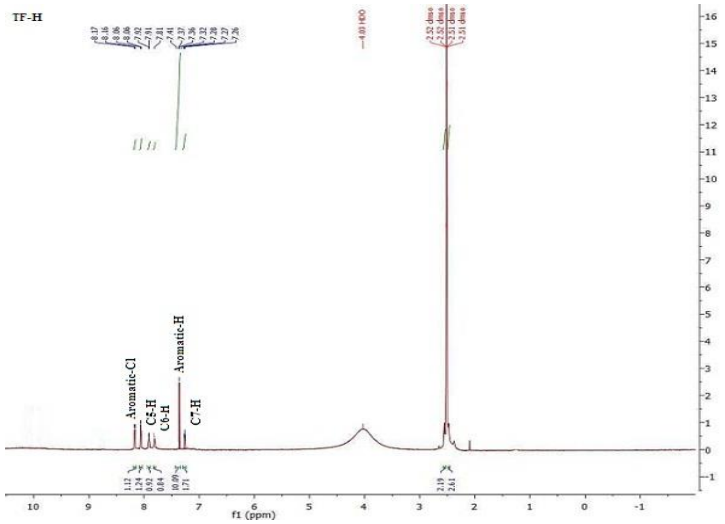

FIGURE 16 ^{1}H-NMR spectrum of ligand (L)

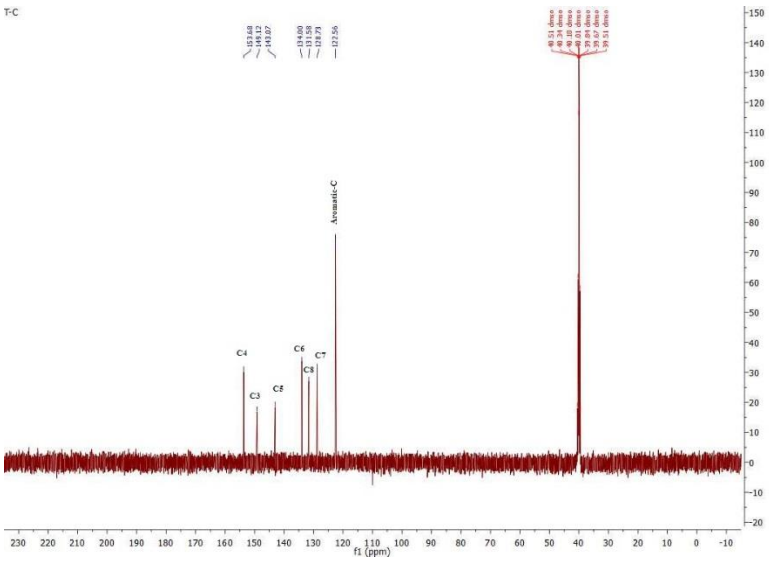

FIGURE 17 ^{13}C-NMR spectrum of Schiff base (A)

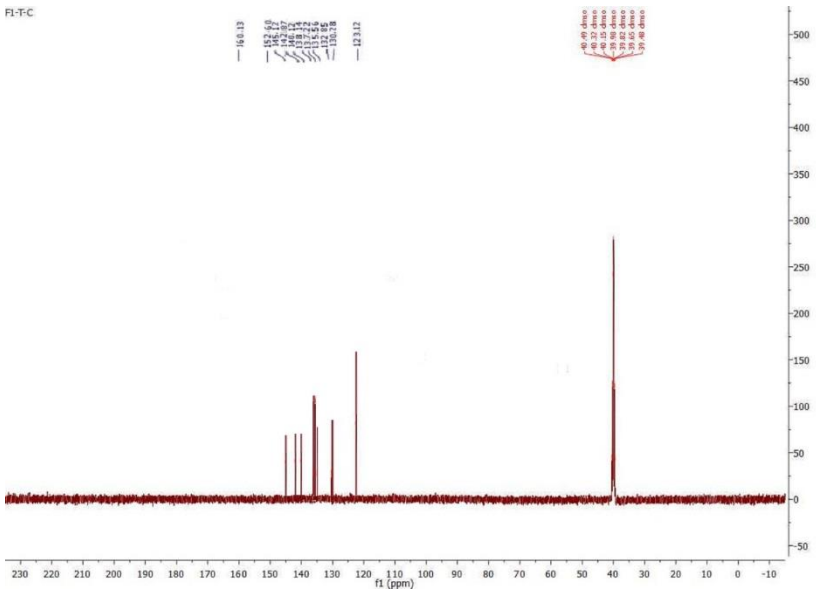

FIGURE 18 ^{13}C-NMR spectrum of ligand (L)

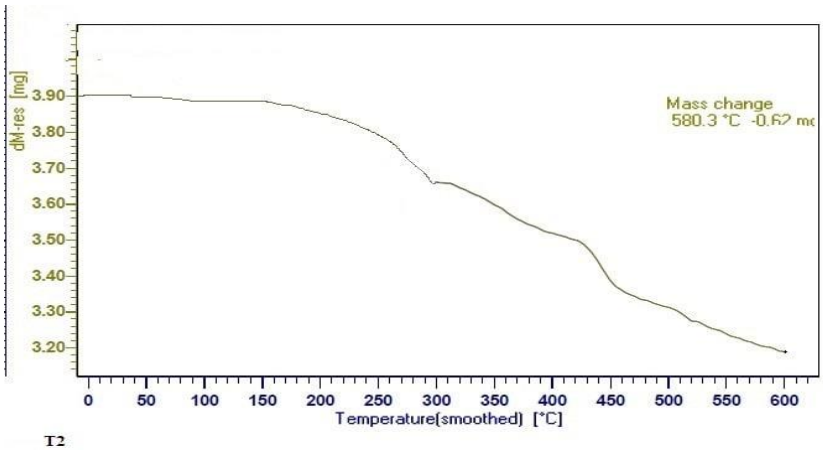

FIGURE 19 TG curve of complex (1)

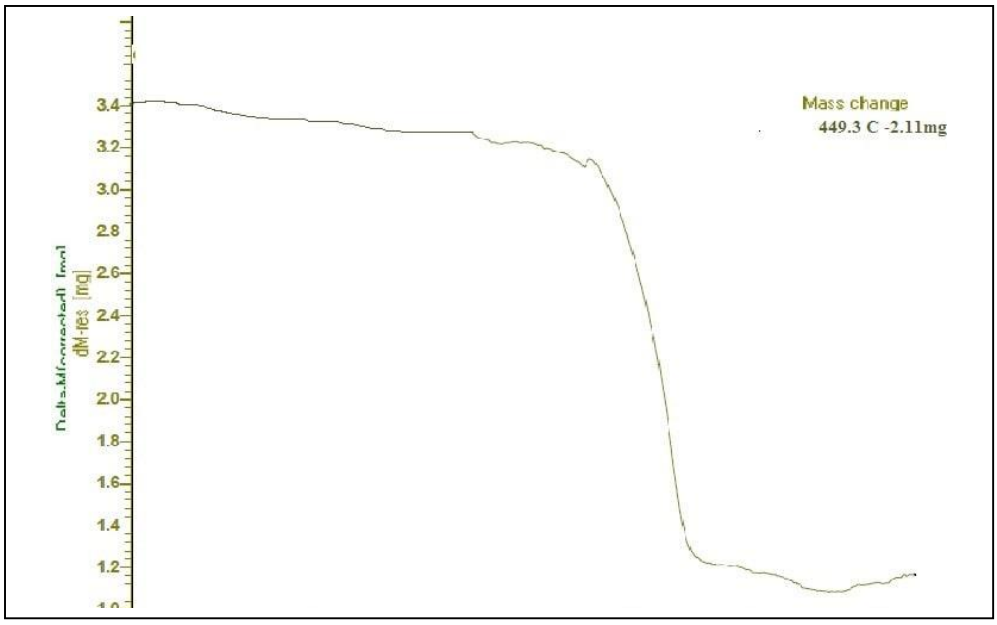

FIGURE 20 TG curve of complex (2)

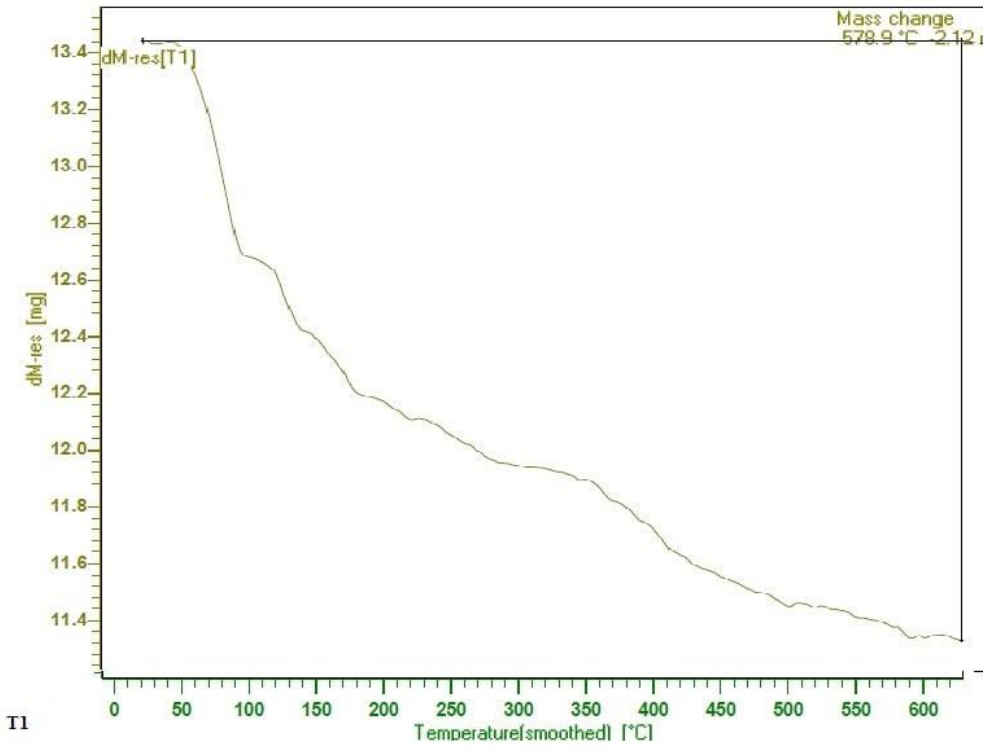

FIGURE 21 TG curve of complex (3)

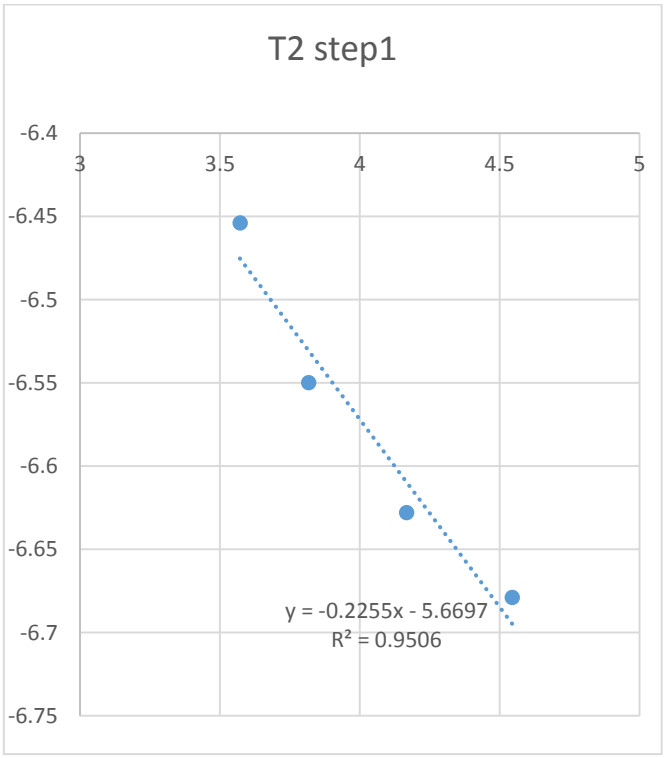

FIGURE 22 Coast-Redfern of $[Cu(L)]Cl_2$ .Step1

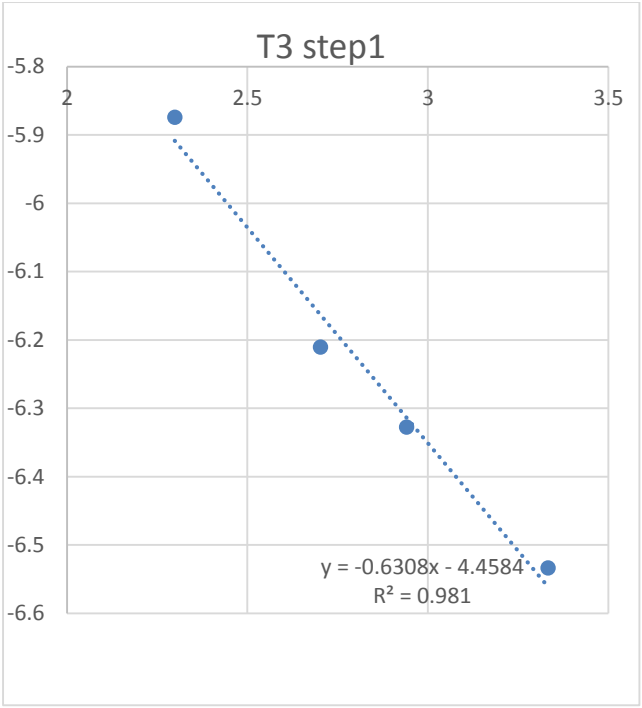

FIGURE 23 Coast-Redfern of $[Ni(L)]Cl_2$ .Step1

Conclusion

The structures of formazan and its metal complexes of Cu(ll), Co(ll) and Ni(ll) were proven by various techniques. The molar conductance showed that all these complexes were electrolytes, while the magnetic measurements showed that they had para-magnetic properties with sp^3 hybridization. The thermal analysis showed that the decomposition process was endothermic, the complexes were more ordered than the reactants, the steps were non-spontaneous and the activation energy in the second step was higher than that of first step, suggesting that the dehydrated complexes were more stable.

Conflicts of interest

There are no conflicts to declare.

Acknowledgments

The authors express their sincere thanks to College of Education for Pure Sciences in University of Basrah. We extent our hearty thanks to the Management of Iran Centre in University of Tehran.

Orcid:

Haneen H. Talib: https://orcid.org/0000-0002-4828-0107

Jasim M. Alshawi: https://orcid.org/0000-0002-2339-2102

References

[1] A.S. Shawali, N.A. Samy, *J. Adv. Res.*, **2015**, *6*, 241-254. [CrossRef], [Google Scholar], [Publisher]

[2] Y. AIbrahim, A.A. Abbas, A.H.M. Elwahy, *J Heterocycl Chem.*, **2004**, *41*, 135-49. [CrossRef], [Google Scholar], [Publisher]

[3] B.I. Buzykin, *Chem. Heterocycle. Compd*, **2010**, *46*, 1043-1062. [CrossRef], [Google Scholar], [Publisher]

[4] D.E. Berry, R.G. Hicks, J.B. Gilroy, *J. Chem. Educ.,* **2009**, *86*, 76-79. [CrossRef], [Google Scholar], [Publisher]

[5] I. Frysova, V. Ruzickova, J. Slouka, T. Gucky, *Acta Univ Palacki Olomuc Fac Rerum Nat, Chem*, **2005**, *44*, 55-61. [Pdf], [Google Scholar], [Publisher]

[6] H. Senoz, *Hacettepe J. Biol. Chem.,* **2012**, *40*, 293-301. [Pdf], [Google Scholar], [Publisher]
[7] Y. Guifa, L. Yiming, *Chemical Reagents*, **1958**, *5*, 6.
[8] P. Thangavelu, S. Chellappa, S. Thangavel, *Int. J. Pharm. Sci.*, **2018**, *10*, 56-61. [CrossRef], [Google Scholar], [Publisher]
[9] T.A. Khattab, K.M. Haggag, *Egypt. J. Chem,* **2017**, 33-40. [CrossRef], [Google Scholar], [Publisher]
[10] Y.H. Al-Araji, J.K. Shneine, A.A. Ahmed, *IJRPC*, **2015**, *5*, 41-76. [Pdf], [Google Scholar], [Publisher]
[11] S. Kumar, R. Sharma, Nitika, *World J. Pharm. Res.*, **2017**, *6*, 800-841. [CrossRef], [Publisher]
[12] M.T. Murali, M. Agarwal, V.K. Sexena, S.K. Bajpai, M.M. Joshi, *Indian J. Pharm. Sci.,* **1995**, *57*, 113-116. [Pdf], [Google Scholar], [Publisher]
[13] R. Kalsi, K. Pande, T.N. Bhalla, S.S. Parmar, J.P. Barthwal, *Pharmacology*, **1988**, *37*, 218-24. [CrossRef], [Google Scholar], [Publisher]
[14] S.B. Chavan, S.B. Zangade, Y. Vibhute, Archana, Y.B. Vibhute, *Res. J. Pharm. Biol. Chem. Sci.,* **2012**, *3*, 262-269. [Google Scholar], [Publisher]
[15] S.D. Bhardwaj, V.S. Jolly, *Chem. Asian J.*, **1997**, *9*, 48-51
[16] K.G. Desai, K.R. Desai, *J. Heterocycl. Chem.*, **2006**, *43*, 1083-1089. [CrossRef], [Google Scholar], [Publisher]
[17] S.k. Yassin, J.M. Alshawi, Z.A.M. Salih, *Egypt. J. Chem.,* **2020**, *63*, 4005-4016. [CrossRef], [Google Scholar], [Publisher]
[18] S.K. Yassin, J.M. Alshawi, Z.A.M. Salih, *Orient. J. Chem.*, **2020**, *36*, 940-945. [CrossRef], [Google Scholar], [Publisher]
[19] F. Erol, N. Sarikavakli, *European Journal of Science and Technology*, **2018**, *14*, 315-322. [CrossRef], [Google Scholar], [Publisher]
[20] D.A. Brown, H. Bogge, G.N. Lipunova, A. Muller, W. Plass, K.G. Walsh, *Inorganica Chimica Acta*, **1998**, *280*, 30-38. [CrossRef], [Google Scholar], [Publisher]
[21] N.L. Mohammed, J.M.S. Al-Shawi, M.J. Kadhim, *Int. J. Sci. Eng. Res.*, **2019**, *7*, 31-40. [Pdf], [Publisher]
[22] J.S. Hadi, Z.A. Abdulnabi, A.M. Dhumed, *European Journal of chemistry*, **2017**, *8*(3), 252-257. [CrossRef], [Google Scholar], [Publisher]

How to cite this article: Haneen H. Talib, Jasim M. Alshawi* Thermal stability, synthesis of new formazan complexes derived from thiophene-2-carboxaldehyde. *Eurasian Chemical Communications*, 2021, 3(12), 938-952. **Link:** http://www.echemcom.com/article_140329.html